



# 1 CryoSCAPE: Scalable Immune Profiling Using 2 Cryopreserved Whole Blood for Multi-omic 3 Single Cell and Functional Assays

4  
5  
6 Alexander T. Heubeck<sup>1,\*</sup>, Cole Phalen<sup>1</sup>, Neel Kaul<sup>1</sup>, Peter J. Wittig<sup>1</sup>,  
7 Jessica Garber<sup>1</sup>, Morgan Weiss<sup>2</sup>, Palak C. Genge<sup>1</sup>, Zachary Thomson<sup>1</sup>,  
8 Claire Gustafson<sup>1</sup>, Julian Reading<sup>1</sup> & Peter J. Skene<sup>1,\*</sup>

9

10 <sup>1</sup>*Allen Institute for Immunology, Seattle, Washington, U.S.A.*

11 <sup>2</sup>*Western University of Health Sciences, College of Osteopathic Medicine of the Pacific*

12 *Northwest, Lebanon, Oregon, U.S.A.*

13 *\*Corresponding Authors*

## 14 Abstract

### 15 Background

16 The field of single cell technologies has rapidly advanced our comprehension of the human  
17 immune system, offering unprecedented insights into cellular heterogeneity and immune  
18 function. While cryopreserved peripheral blood mononuclear cell (PBMC) samples enable deep  
19 characterization of immune cells, challenges in clinical isolation and preservation limit their  
20 application in underserved communities with limited access to research facilities. We present  
21 CryoSCAPE (Cryopreservation for Scalable Cellular And Proteomic Exploration), a scalable  
22 method for immune studies of human PBMC with multi-omic single cell assays using direct  
23 cryopreservation of whole blood.

### 24 Results

25 Comparative analyses of matched human PBMC from cryopreserved whole blood and density  
26 gradient isolation demonstrate the efficacy of this methodology in capturing cell proportions and  
27 molecular features. The method was then optimized and verified for high sample throughput  
28 using fixed single cell RNA sequencing and liquid handling automation with a single batch of 60  
29 cryopreserved whole blood samples. Additionally, cryopreserved whole blood was  
30 demonstrated to be compatible with functional assays, enabling this sample preservation  
31 method for clinical research.

### 32 Conclusions

33 The CryoSCAPE method, optimized for scalability and cost-effectiveness, allows for high-  
34 throughput single cell RNA sequencing and functional assays while minimizing sample handling  
35 challenges. Utilization of this method in the clinic has the potential to democratize access to

36 single-cell assays and enhance our understanding of immune function across diverse  
37 populations.

## 38 Background

39 The rapidly evolving field of single cell technologies has become a central component in  
40 advancing our understanding of the human immune system, revealing the cellular heterogeneity  
41 that underlies immune function. Analyzing protein abundance, gene expression, and epigenetics  
42 at single-cell resolution provides new observations into cell phenotypes and states in both  
43 health and disease, with the potential to identify novel biomarkers and therapeutic targets<sup>1,2</sup>. A  
44 critical aspect to utilizing these tools is the sourcing, isolation, and preservation of clinical  
45 samples from patients for studies performed downstream in research laboratories. Peripheral  
46 blood mononuclear cells (PBMCs) are one of the most common sample types for studying the  
47 immune system<sup>3</sup> and serve as a valuable source for such studies, offering a snapshot of the  
48 immune system at the time of sample collection that can be cryopreserved for extended periods  
49 and analyzed using state of the art technologies years later. Cryopreserved PBMC samples also  
50 enable functional assays many years after collection, including cellular stimulations and genetic  
51 manipulations<sup>4,5,6,7</sup>.

52

53 Although isolating and cryopreserving PBMCs is the current standard method in immunology  
54 research studies, there are challenges related to PBMC isolation and preservation in the clinic  
55 that limit the scope of sample collection. In the clinical isolation of PBMCs for immune studies,  
56 the primary obstacles stem from the time and method sensitive nature of the process. Delays in  
57 sample processing of more than 4 hours after blood draw can have profound changes in the  
58 single-cell transcriptome and composition of the plasma proteome<sup>8,9</sup>. Standardizing sample  
59 handling methods becomes particularly challenging in clinical cohorts across multiple sites,

60 introducing variability that may obscure important biological differences<sup>7</sup>. Additionally, limited  
61 access to specialized equipment and trained personnel acts as a barrier, preventing many  
62 clinical sites from participating in studies that require PBMC isolation. This limitation, especially  
63 prevalent in low-income or underserved areas, hinders access to diverse patient samples<sup>10,11</sup>.  
64 Commercial options that address these issues with point of collection fixation exist, but were  
65 largely designed for flow cytometry and are not compatible with most next generation  
66 sequencing assays<sup>12,13</sup>. Other approaches utilizing cryopreservation of whole blood have shown  
67 extension to single cell RNA sequencing but without faithfully maintaining cell proportions or  
68 demonstration of functional assays<sup>14</sup>. Addressing these obstacles is crucial for enabling more  
69 impactful analysis of human immunology, with the potential to expand current studies to a  
70 broader and more diverse population.

71  
72 In addition to the challenges of human PBMC sample collection and preservation, the current  
73 constraints of single-cell technologies pose significant obstacles to conducting large-scale  
74 studies in many research settings. In the case of single cell sequencing, prohibitively high costs  
75 and method complexity often restrict the number of patient samples that can be feasibly  
76 analyzed and diminish the efficacy of clinical datasets<sup>15</sup>. Many single-cell assays also  
77 necessitate the use of live cells, thereby limiting access to in vitro time course studies that are  
78 optimally conducted using fixatives to capture cell states at precise time points<sup>16,17</sup>. Improving  
79 upon the cell handling and assay scalability limitations of single cell sequencing, as well as the  
80 challenges in clinical PBMC preservation, would democratize access to these important  
81 technologies, unlocking new possibilities for clinical discovery and translational impact.

82  
83 To address the challenges of conventional human immune studies, we optimized an accessible  
84 sample collection methodology with a scalable and cost effective method for generating single  
85 cell sequencing datasets combined with functional assays using human PBMCs called

86 CryoSCAPE (Cryopreservation for Scalable Cellular And Proteomic Exploration). This approach  
87 utilizes direct cryopreservation of whole blood using freezing media containing DMSO in a  
88 similar fashion to standard PBMC cryopreservation. Red blood cell and granulocyte removal  
89 that would usually be completed by density gradient PBMC isolation in the clinic are performed  
90 on the samples at the research site to reduce handling time in the clinic and enable scalable  
91 multiplexed scRNA-seq readouts. To demonstrate the utility of CryoSCAPE, we show that  
92 relative cell proportions, single cell gene expression, single cell protein expression and  
93 epigenetic profiling of cryopreserved density gradient isolated PBMCs and cryopreserved whole  
94 blood were highly comparable. The method was also optimized for high throughput and low cost  
95 sample processing through automation, as demonstrated by analysis of highly multiplexed fixed  
96 scRNA-seq results from sixty cryopreserved whole blood samples in a single batch. In addition  
97 to multi-omic single cell readouts, the developed method enables stimulation of PBMC from  
98 cryopreserved whole blood, verified through in vitro immune stimulation assays. The integration  
99 of this methodology into research and clinical settings has the potential to broaden the  
100 application of single-cell assays, especially in underrepresented communities, and enhance our  
101 understanding of immune function across diverse populations.

## 102 Results

103 Cryopreserved whole blood samples demonstrate comparable results to  
104 cryopreserved density gradient isolated PBMC using single cell multi-omics  
105 readouts  
106 To improve accessibility to clinical sample collection of human peripheral blood mononuclear  
107 cells (PBMCs), we optimized a whole blood cryopreservation method for use in clinical settings

108 without access to equipment required for density gradient PBMC isolation (Fig. 1a). The method  
109 uses a freezing media composed of 15% dimethyl sulfoxide (DMSO) as a cryopreservation  
110 agent, diluted with CryoStor preservation media as a serum-free protein supplement. In this  
111 method, whole blood drawn in sodium heparin tubes is combined 1:1 with 15% DMSO freezing  
112 media in 5 mL cryopreservation tubes to achieve a final DMSO concentration of 7.5%. The  
113 whole blood is thoroughly mixed in the freezing media by inverting the tubes, then transferred  
114 into a slow freezing container. Samples can be safely stored at -80°C in a freezer or in dry ice  
115 before being shipped to the research laboratory for long term storage in liquid nitrogen. This  
116 simple and immediate cryopreservation method allows for preservation of PBMCs with no delay  
117 in processing time, and without specialized technicians or equipment, as required with standard  
118 PBMC density gradient isolation methods.

119  
120 By simplifying the clinical site requirements for sample cryopreservation, additional processing  
121 at the research site is required to fully enrich PBMCs for single cell assays. Once the  
122 cryopreserved whole samples have been thawed in a 37°C water bath, red blood cells (RBCs)  
123 are removed using a RBC lysis buffer, as they can reduce gene detection in scRNA-seq  
124 readouts<sup>18</sup>. Granulocytes from cryopreserved whole blood samples typically have very low  
125 viability upon thaw, and can cause cell clumping through release of DNA and lysosomal  
126 enzymes upon thawing<sup>13,18</sup>. Samples are incubated with DNase I solution to reduce clumping  
127 prior to further enrichment<sup>19</sup>. Granulocytes, dead cells, and other debris that are removed with  
128 density gradient PBMC isolation must also be removed from the samples, typically using a cell  
129 isolation method such as fluorescence-activated cell sorting (FACS). While this additional  
130 enrichment increases the workload at the research site, removing that responsibility from the  
131 clinical side enables more sample collection centers to participate in immunological studies.

132

133 This whole blood cryopreservation technique was evaluated for compatibility with multi-omic  
134 sequencing assays through a comparative analysis of PBMCs preserved using the  
135 cryopreserved whole blood method versus the conventional density gradient PBMC isolation  
136 approach (Fig. 1a). Whole blood samples were obtained from three donors and subjected to  
137 cryopreservation using both the whole blood and density gradient PBMC cryopreservation  
138 methods, with subsequent storage for a minimum of 6 months. Analysis of PBMCs from each  
139 method included enrichment with FACS (Supplement Fig. 1) followed by deep molecular  
140 characterization via scRNA-seq, scCITE-seq, and bulk ATAC-seq, to evaluate differences in  
141 gene expression, surface protein expression, and chromatin accessibility, respectively. Gene  
142 expression results from healthy donors (n=3) were captured using the 10x Genomics Flex single  
143 cell fixed RNA-seq kit, resulting in data from 21,023 and 17,780 single cells generated from  
144 cryopreserved whole blood and density gradient isolated PBMCs, respectively. Protein  
145 expression was measured using CITE-seq antibody derived tags (ADTs) in conjunction with the  
146 10x Flex single cell fixed kit, for matched gene and protein results from the same single cells.  
147 Both the cryopreserved whole blood and density gradient isolated PBMC methods produced  
148 high quality data with comparable unique gene expression molecular identifiers (UMIs) per cell,  
149 median gene counts per cell, and antibody derived tags (ADTs) UMIs per cell (Fig 1b). After  
150 removal of doublets and normalization, samples were labeled using Seurat label transfer to  
151 identify 7 major immune cell types (CD4 T Cells, CD8 T Cells, Other T Cells, B Cells, NK Cells,  
152 Monocytes, and Dendritic Cells (DCs)) based on gene expression (Fig. 1c). Relative population  
153 frequencies of the major cell types displayed high correlation between cryopreserved methods  
154 ( $R=0.970$ ,  $p<0.001$ ), indicating no reduction of specific cell populations in cryopreserved whole  
155 blood.  
156  
157 Similarity between cryopreservation methods is further confirmed with combined donor Uniform  
158 Manifold Approximation Projections (UMAPs) clustered on gene expression, showing high

159 similarity of cell type clustering (Fig 1d). To assess cell type specific differences, the average  
160 expression of the highest expressing genes per cell type were compared across  
161 cryopreservation methods (142 total genes). Gene expression was highly correlated for all cell  
162 types ( $R>0.979$ ), again highlighting the similarity of gene expression between cryopreserved  
163 whole blood and density gradient isolated PBMC. Protein expression UMAPs were also labeled  
164 using the same major cell type label transfers, demonstrating a highly similar surface protein  
165 profile between the cryopreservation methods (Fig. 1e). Cell type specific protein differences  
166 were evaluated by comparing the average expression of ADTs with expression levels above  
167 isotype controls (116 total proteins). Similar to the gene expression data, protein expression  
168 was highly correlated for all cell types ( $R>0.981$ ), further demonstrating the viability of using  
169 cryopreserved whole blood for single cell sequencing readouts with no loss of resolution  
170 compared to standard PBMC cryopreservation methods.

171  
172 In addition to gene and protein expression, epigenetic profiling is an important approach to  
173 measure enhancer and transcription factor accessibility but has also been shown to be sensitive  
174 to delays in PBMC processing<sup>17</sup>. Chromatin accessibility was evaluated using ATAC-seq on  
175 bulk cell populations in both whole blood and density gradient isolated PBMC cryopreservation  
176 methods. The profiles of cryopreserved whole blood and density gradient isolated PBMCs show  
177 similar profiles with enrichment around transcriptional start sites (TSS) at a representative  
178 region of the genome (Fig. 1f, Supplement Table 2). To evaluate this on a genome wide scale,  
179 all libraries were equally downsampled to 14 million total mapped sequenced reads and total  
180 coverage of Tn5 footprints summed across all TSS. Clear enrichment across TSS regions was  
181 observed in both sample cryopreservation methods. Reduced peak height at the TSS in  
182 cryopreserved whole blood samples was observed, with the ratio of the maximum peak height  
183 near the TSS between cryopreserved whole blood and density gradient isolated PBMCs varying  
184 between samples (0.99, 0.56 and 0.59 in Donors 1, 2 and 3, respectively). This decreased

185 signal to noise ratio in the cryopreserved whole blood may be due to extracellular debris  
186 generated from the whole blood cryopreservation workflow, but still allows for interpretation of  
187 chromatin accessibility. The successful interrogation of cryopreserved whole blood samples  
188 using these multi-omic assays enables CryoSCAPE to be used for simpler sample collection for  
189 immunological studies.

190 **Scaling cryopreserved whole blood sample throughput using 10x Flex  
191 scRNA-seq technology and automation**

192 Analysis of circulating PBMC using scRNA-seq is a powerful tool to gain insight into the human  
193 transcriptome; however, the cost and scalability of these assays still remains a significant  
194 obstacle to more widespread adoption. Droplet based single cell sequencing technologies that  
195 utilize a poly-A based mRNA capture method for full transcriptome coverage have improved  
196 single cell throughput in recent years, but have yet to lower the assay cost enough to enable  
197 large scale studies<sup>20</sup>. A recently released method for measuring gene expression from mRNA of  
198 fixed cells, the Chromium Single Cell Gene Expression Flex kit from 10x Genomics, employs a  
199 paraformaldehyde cell fixation step followed by the hybridization of a barcoded probe panel to  
200 capture transcriptional activity. With the barcoded probe panel utilized in 10x Flex scRNA-seq,  
201 doublets can be resolved in-silico, permitting a higher cell loading concentration and assay  
202 throughput, significantly driving down the cost per cell. Further cost efficiencies can be found  
203 with workflow automation allowing for the analysis of batches of 64 or more samples, providing  
204 an 6-fold cost reduction per sample (\$526 Flex vs. \$3,604 3' v3.1, Supplement Table 3). In  
205 addition to the cost advantages due to multiplexing, the 10x Flex scRNA-seq method also  
206 displays improved sensitivity and is more compatible with high throughput processing by  
207 incorporating additional stop points and a less complex overall workflow.

208

209 To evaluate the 10x Flex scRNA-seq as a higher throughput and cost effective alternative to 10x  
210 3' v3.1 scRNA-seq, gene expression profiles generated from each method were compared  
211 using density gradient isolated PBMCs from healthy donors (n=3). The 10x Flex scRNA-seq kit  
212 showed improved assay sensitivity, detecting ~70% more genes and equal numbers of unique  
213 molecular identifiers (UMIs) from 75% of captured reads compared to the 10x 3' v3.1 kit despite  
214 libraries being sequenced at ~75% read depth (Fig. 2a). The 10x Flex method also shows  
215 improved detection of genes per cell ( $2746 \pm 14$  s.e.m.) over 10x 3' v3.1 ( $1527 \pm 19$  s.e.m.) (Fig.  
216 2b). Despite the differences in gene detection efficiency, concordant cell population frequencies  
217 were observed based on cell label transfer between 10x Flex and 10x 3' v3.1 ( $R=0.995$ ,  
218  $pval<0.001$ ), suggesting that there was no observable effect of probe hybridization bias towards  
219 a specific cell type leading to differences in cell type labeling across 3 donors (Fig. 2c).

220  
221 The performance of the 10x Flex scRNASeq kit was evaluated in conjunction with the developed  
222 whole blood cryopreservation method to enable a low cost-scalable method for high throughput  
223 single cell transcriptome analysis. While FACS is a highly effective method for isolating high  
224 purity cells for scRNA-seq, sorting cryopreserved whole blood samples can take up to 15  
225 minutes per sample (24 hours for 96 samples) due to high debris content, severely limiting the  
226 throughput for larger batches of samples. Negative selection with magnetic bead enrichment,  
227 where non-target cells and debris are bound with magnetic beads and removed with a strong  
228 magnet, is an alternative purification method that can be easily scaled. Magnetic bead  
229 enrichment and FACS methods were compared for isolating PBMCs from cryopreserved whole  
230 blood (n=3) and density gradient isolated PBMCs (n=1), measured by 10x Flex scRNA-seq  
231 quality metrics and enrichment of PBMCs using flow cytometry analysis (Fig. 2d). As expected,  
232 FACS enrichment of viable leukocytes produced comparable UMIs and genes per cell between  
233 samples isolated from cryopreserved whole blood and density gradient isolated PBMCs. The  
234 initial magnetic bead enrichment method was tested using a single round of bead binding of a

235 human dead cell removal kit to remove the low viability granulocyte compartment of the  
236 cryopreserved whole blood. Samples enriched using this magnetic bead depletion showed high  
237 quality metrics using the 10x 3' v3.1 kit (Supplement Fig. 2). However, despite enriching the  
238 PBMCs from cryopreserved whole blood to at least 95% purity, a significant loss in 10x Flex  
239 library quality was observed, as less than half of the genes per cell were detected compared to  
240 cells enriched from density isolated PBMCs using the same method (Fig. 2d).

241  
242 The magnetic bead enrichment method was improved by adding PE conjugated antibodies  
243 targeting CD15 and CD66b followed by binding of anti-PE magnetic beads in addition to the  
244 dead cell removal beads to target any remaining granulocytes in the samples. This step was  
245 then repeated for a total of two rounds to further isolate the target cells to greater than 99%  
246 purity, which closely matched the purity of FACS sorted cells (Fig. 2e). This additional removal  
247 of granulocytes improved the genes per cell detected in the magnetic bead depleted samples to  
248 the same level as the FACS sorted or density gradient isolated PBMC samples, demonstrating  
249 the utility of this scalable sample enrichment method with the 10x Flex scRNAseq assay (Fig.  
250 2e). A cryopreserved whole blood sample with no enrichment included as a control produced  
251 extremely low detection of genes per cell, further highlighting the need to completely remove all  
252 granulocytes from a sample before using the 10x Flex scRNA-seq chemistry.

253  
254 Development of the scalability of the method continued with adaptation of the magnetic bead  
255 enrichment and the 10x Flex scRNA-seq assay from a tube based method into a 96 well plate  
256 format with reduced reaction volumes to enable high throughput analysis (Fig. 3a). This format  
257 also allowed for the integration of liquid handling automation to enable a single operator to  
258 process up to 96 samples simultaneously. This workflow was evaluated by analyzing matching  
259 cryopreserved whole blood (n=7) and density gradient isolated PBMC (n=1) samples using the  
260 automated plate format magnetic bead enrichment and FACS enrichment methods followed by

261 10x Flex scRNA-seq, resulting in 110,594 (Bead Enrichment) and 103,501 (FACS) individual  
262 recovered cells. Library quality was assessed by comparing genes per cell as recovered using  
263 the plate based magnetic bead enrichment ( $1743 \pm 59$  s.e.m.) and FACS ( $1762 \pm 99$  s.e.m.)  
264 methods (Fig. 3b). UMAPs of gene expression overlaid with major immune cell type labeling  
265 showed similar clustering between the two enrichment methods, and cell type proportions show  
266 high correlation ( $R=0.988$ ,  $p<0.001$ ), indicating no significant differences in PBMC frequency in  
267 either enrichment method (Fig. 3c). Differences in differentially expressed genes between  
268 donors were conserved in both enrichment methods, and the gene expression between  
269 enrichment methods are highly correlated ( $R>0.988$ ) (Fig. 3d). The magnetic bead depletion in  
270 plate format produced high quality results comparable to FACS enrichment, enabling us to  
271 analyze samples with much higher throughput at significantly reduced cost.

272

273 Utilizing multiplexed scRNA-seq, plate based magnetic bead enrichment, and automated  
274 sample handling enabled us to develop a high throughput, cost efficient workflow for gene  
275 expression analysis on fixed cells from cryopreserved whole blood (Fig. 4a). To verify this  
276 workflow, 60 cryopreserved whole blood samples and 1 PBMC control were processed  
277 simultaneously, generating a dataset containing scRNA-seq data from 429,366 single cells (Fig.  
278 4b). Samples were divided into 4 pools of 16 samples, where each pool was thawed by a  
279 separate operator. Within each pool, 3 replicate cryopreserved whole blood tubes from 5  
280 individual donors were analyzed in order to evaluate consistency within and between pools. A  
281 single density gradient isolated PBMC sample was divided into 4 wells and added to each  
282 sample pool as a bridging control to further assess technical variance.

283

284 Individual cryopreserved whole blood replicates exhibited consistent gene expression results  
285 with high correlation measured between replicates of the same donor ( $R>0.980$ ). UMAPs of  
286 gene expression results between operators also display highly similar clustering (Fig. 4b,

287 Supplement Figure 3). Variance decomposition analysis was performed to evaluate  
288 contributions of study variables to total variance of individual genes (Fig. 4c). Sample technical  
289 replicate and operator features were found to have low impact on the variance in gene  
290 expression (<10%). While some variance can be attributed to sex-linked genes from male and  
291 female donors (2 male, 6 female), the majority of gene expression variance can be attributed to  
292 biological factors, rather than deviations introduced by the workflow<sup>21</sup>. Within a single donor,  
293 gene expression from six housekeeping genes<sup>22</sup> (ACTB, ARF1, B2M, CWC15, UBC, YWAHZ)  
294 across the four operators displayed consistent gene expression (coefficient of variation<5%),  
295 again demonstrating the methods reproducibility across replicates (Fig. 4d). Within the entire  
296 batch of samples, average gene expression was highly correlated between technical replicates  
297 ( $R>0.970$ ), while conserving differences between donors (Fig. 4e). The generation of high  
298 quality and robust technical replicate data using this workflow demonstrates both the  
299 consistency of cryopreserved whole blood samples, even with handling by different operators,  
300 and the feasibility of using automation to increase sample throughput and reduce cost.

301 Enabling high throughput functional assays on cryopreserved whole blood  
302 A crucial component to immunological studies involving PBMCs is the ability to perturb collected  
303 cells and observe their response to stimuli with a variety of readouts. In addition to single cell  
304 readouts, we evaluated if samples preserved with the described cryopreserved whole blood  
305 method are compatible with functional assays at scale using well characterized stimulations that  
306 target different immune cell types. Cryopreserved whole blood (n=3) and density gradient  
307 isolated PBMC (n=1) samples were thawed and enriched for PBMCs using the automated  
308 magnetic bead depletion described previously. The transcriptional response of each sample to  
309 three stimulation conditions was measured, including phorbol 12-myristate 13-acetate (PMA)  
310 with ionomycin, resiquimod (R848), and CD3/CD28 T cell activation beads against unstimulated

311 cells (Fig. 5a). After a four hour incubation period, cells were immediately fixed to preserve the  
312 transcriptional state, and then analyzed using 10x Flex scRNA-seq.

313

314 UMAP projections of the gene expression data from these functional assays reveal specific cell  
315 types grouping in multiple clusters, representing distinct responses to stimulation (Fig. 5b). Cells  
316 from all donors also clustered together in response to each specific stimulation, demonstrating  
317 the preservation of cellular response in cryopreserved whole blood compared to density  
318 gradient isolated PBMC (Fig. 5c, Supplement Fig. 4). Analysis of each stimulation condition  
319 against matched unstimulated cells also revealed a high degree of concordance of differentially  
320 expressed genes (DEGs) for all donors irrespective of cryopreservation method (67% PMA +  
321 Iono., 52% R848, 42% CD3/CD28 Beads) (Fig. 5d). Some DEGs remain specific to individual  
322 donors, including a strong DEG response signature to CD3/CD28 Beads occurring in one  
323 cryopreserved whole blood donor, indicative of the maintenance of biological differences  
324 between donors in the whole blood cryopreservation method.

325

326 A deeper look into specific activation marker genes reveals classical cell type specific  
327 responses in all donors, including CD8 T cell response to PMA and Ionomycin, B cell response  
328 to R848, and CD4 T cell response to CD3/CD28 activation beads (Fig. 5E)<sup>23,24</sup>. Unbiased  
329 analysis of the highest upregulated and downregulated genes also show comparable patterns  
330 between all cryopreserved whole blood and density gradient isolated PBMC donors.

331 Confirmation of these expected gene signatures and cell type specific responses enables the  
332 use of this cryopreserved whole blood method for scalable functional assays, and further  
333 validates the importance of this method for large scale studies or settings where PBMC  
334 processing is operationally unfeasible.

## 335 Discussion

336 While technology to interrogate the immune system continues to rapidly innovate, sample  
337 preservation methods have had limited improvements to enable large scale clinical  
338 investigations and remain a barrier to studying underserved communities remote from research  
339 facilities. Density gradient isolation and cryopreservation of PBMCs have been the gold  
340 standard for longitudinal immune cell studies for decades, but the drawbacks to this method,  
341 including laboratory requirements and processing delays, have persisted. Alternative methods  
342 of preserving PBMCs using fixation do address these issues, but only allow for analysis of the  
343 samples at the time of blood draw and prevent use in functional assays. We developed a  
344 simplified workflow for cryopreservation of whole blood that enables immediate freezing of  
345 whole blood draws, allows for generation of high quality data from sequencing readouts, and  
346 facilitates functional assays on preserved cells. The CryoSCAPE method enables clinical  
347 studies using blood draws to collect and preserve samples immediately, only requiring cold  
348 storage (-80°C freezer or dry ice) with minimal training.

349

350 Similar whole blood cryopreservation methods have been described previously and  
351 demonstrated this whole blood cryopreservation method is viable for flow cytometry and scRNA-  
352 seq analysis, but without faithfully maintaining cell proportions or demonstration with large scale  
353 studies. We presented a method for whole blood cryopreservation that is compatible with deep  
354 molecular profiling including highly multiplexed fixed RNA-seq, CITE-seq, and ATAC-seq.  
355 Additionally, the ability to apply RNA-seq and CITE-seq on fixed cells from this cryopreservation  
356 method increases the throughput and reduces the cost of running these assays. Other  
357 methodologies using DMSO whole blood cryopreservation have indicated loss of monocytes  
358 compared to matched PBMC samples due to use of red blood cell depletion beads that remove  
359 platelets bound to monocytes, and require high amounts of EDTA to be supplemented to

360 prevent this effect<sup>14</sup>. The use of an RBC lysis buffer in this method to remove red blood cells  
361 has no impact on cell type frequency or transcriptional readouts.

362

363 We also demonstrated that this method of cryopreservation is compatible with high throughput  
364 studies utilizing liquid handling automation, including functional studies incorporating large  
365 numbers of conditions or samples. Use of fixation prior to scRNA-seq can also allow for very  
366 short and long time scale functional assays, further improving upon other cryopreservation  
367 methods that fix the cells at the time of collection, or have only been demonstrated to work with  
368 unfixed sequencing assays. In conclusion, our study presents a significant advancement in  
369 sample preservation methods and post-thaw processing for large-scale clinical investigations  
370 focusing on peripheral blood mononuclear cells (PBMCs). Our proposed method of  
371 cryopreserving whole blood addresses clinical sample collection challenges by enabling  
372 immediate freezing of blood samples, thus streamlining workflow and facilitating high-quality  
373 data generation across various sequencing readout assays. Moreover, our approach is not only  
374 compatible with functional assays but also demonstrates reproducibility and correlation across  
375 multiple sequencing pools and sample thaw operators.

376 **Conclusions**

377 Incorporation of this cryopreservation methodology and high throughput automation into clinical  
378 trials has the potential to transform our understanding of immunology. Simplified blood collection  
379 on the clinical side opens up understudied geographic, economic, racial and ethnic populations  
380 that previously had poor representation in studies due to the inability to reach clinical centers  
381 that could process and cryopreserve PBMCs. Scaling of sample throughput using automation  
382 and targeted multi-omic readouts drastically lowers the cost per sample and allows research  
383 centers to increase the power of their studies. By offering a simplified and efficient alternative to

384 conventional methods, CryoSCAPE opens doors for enhanced research capabilities in  
385 immunology and beyond, promising greater accessibility and reliability in clinical studies utilizing  
386 blood samples.

## 387 Methods

### 388 Sample Collection

389 Whole blood draws were collected with written informed consent under the supervision of an  
390 Institutional Review Board (IRB) Protocol. Whole blood sourced from healthy subjects were  
391 collected by BloodWorks NorthWest (Seattle, WA) and the Benaroya Research Institute  
392 (Seattle, WA) through protocols approved by the relevant institutional review boards  
393 (Supplement Table 1). Blood samples were drawn into blood collection tubes with sodium  
394 heparin, and delivered to the Allen Institute within 4 hours of blood draw and processed  
395 immediately.

### 396 Whole Blood Cryopreservation

397 Cryopreserved whole blood aliquots were generated by combining 2 mLs of fresh whole blood  
398 with 2 mLs of room temperature 15% DMSO freezing media containing CryoStor10 (Biolife  
399 Solutions) supplemented with additional DMSO (Sigma). Whole blood and freezing media was  
400 combined in a 5 mL cryotube, resulting in a final freezing concentration of 7.5% DMSO.  
401 Cryotubes were capped and inverted 10 times to fully mix the blood and freezing media.  
402 Samples were then transferred to a room temperature CoolCell Freezing Container (Corning)  
403 and stored in a -80°C freezer for 24 hours to slow freeze at a rate of 1°C per hour. Frozen  
404 whole blood aliquots were then stored in vapor phase liquid nitrogen.

## 405 PBMC Isolation and Cryopreservation

406 Peripheral blood mononuclear cells (PBMCs) were isolated from whole blood by Ficoll density  
407 gradient (GE Healthcare) centrifugation using SepMate 50mL Isolation tubes (STEMCELL  
408 Technologies) according to the manufacturer's protocol. The PBMC fraction was isolated and  
409 resuspended in CryoStor CS10 (Biolife Solutions) at a concentration of 5 million cells per mL.  
410 PBMC suspensions were distributed in 1 mL cell aliquots into 1.5 mL cryotubes, transferred to  
411 a Corning CoolCell Freezing Container, and stored in a -80°C freezer for 24 hours. Frozen  
412 PBMC aliquots were then stored in vapor phase liquid nitrogen.

## 413 Cryopreserved Whole Blood Thaw

414 Cryopreserved whole blood samples were thawed in a 37°C water bath, transferred into 30 mL  
415 of pre-warmed AIM V media (37°C) (GIBCO), and centrifuged for 10 minutes at 400g (4°C) in a  
416 swinging bucket rotor. Thawed cells were washed with 30 mL of cold AIM V media (4°C) and  
417 centrifuged for 10 minutes at 400g (4°C) in a swinging bucket rotor. To remove red blood cells  
418 (RBC), the thawed samples were resuspended in 10 mL of cold RBC Lysis Buffer (BioLegend)  
419 for 15 minutes (4°C). 20 mL of AIM V media (4°C) was added to quench the lysis reaction, and  
420 then cells were centrifuged for 10 minutes at 400g (4°C). To prevent clumping, thawed cells  
421 were resuspended in 200 µL of 0.2 mg/mL DNase I Solution (STEMCELL Technologies),  
422 incubated at room temperature for 15 minutes. The cells were then washed with 30 mL of cold  
423 AIM V media (4°C) and centrifuged for 10 minutes at 400g (4°C). Individual samples were  
424 resuspended in 250 µL of Dulbecco's phosphate-buffered saline (DPBS) (Costar) for cell  
425 staining for FACS, or in 250 µL of Mojosort Isolation Buffer (BioLegend) for magnetic bead  
426 enrichment.

427 **Cryopreserved PBMC Thaw**

428 Cryopreserved PBMC samples were thawed in a 37°C water bath, transferred into 30 mL of pre-  
429 warmed AIM V media (37°C) (GIBCO), and centrifuged for 10 minutes at 400g (4°C). Thawed  
430 cells were resuspended in 5 mL of cold AIM V (4°C), and 30 µL was removed for counting. The  
431 counting fraction was stained 1:1 with 30 uL of AO/PI solution and counted on a Nexcelom  
432 Cellaca MX cell counter (Supplement Note). Thawed cells were then washed with 25 mL of cold  
433 AIM V media (4°C) and centrifuged for 10 minutes at 400g (4°C). Individual samples were  
434 resuspended in Dulbecco's phosphate-buffered saline (DPBS) (Costar) at a concentration of 10  
435 million cells per mL for cell staining for FACS, or in 250 µL of Mojosort Isolation Buffer  
436 (BioLegend) for granulocyte and dead cell bead enrichment.

437 **FACS and Flow Cytometry Analysis**

438 Fluorescence activated cell sorting (FACS) and flow cytometry analysis were performed using a  
439 3 marker panel including FVS510 Fixable Viability Stain (BD Biosciences), CD45 FITC (Clone  
440 2D1, BioLegend), and CD15 PE (Clone HI98, BioLegend). Samples were stained 1:500 with  
441 FVS510 viability stain in 100 uL total volume for 20 minutes (4°C), and washed once with  
442 Mojosort Isolation Buffer (BioLegend). Samples were then stained with 3 uL each of CD15 PE  
443 and CD45 FITC antibodies in 100 uL total volume for 30 minutes (4°C), and washed twice and  
444 resuspended in Mojosort Isolation Buffer. Viable PBMCs were sorted with a BD FACSaria cell  
445 sorter, gated on FVS510 viability negative, CD15 PE negative, and CD45 FITC positive cells  
446 (Supplement Fig. 1a). Bead enriched cells were analyzed using a Cytek Aurora spectral  
447 cytometer (Supplement Note). Compensation and unmixing controls for each respective  
448 instrument were generated from healthy PBMC samples. Flow Cytometry Standard (FCS) files  
449 from the BD FACSaria cell sorter and the Cytek Aurora spectral cytometer were exported in

450 FCS 3.1 format. Manual gating analysis for figures was generated using FlowJo (BD  
451 Biosciences, v10.10.0).

452 **Magnetic Bead Enrichment**

453 Samples were stained with 5 uL CD15 PE (Clone HI98, BioLegend) and 5uL CD66b PE (Clone  
454 6/40c) in a total volume of 100 uL for 15 minutes (4°C). Stained cells were washed with 100 uL  
455 of 1X Mojosort Isolation Buffer (Biolegend), centrifuged at 400g for 5 min (4°C), resuspended in  
456 100uL of 1X Mojosort Isolation Buffer. Samples were then stained with 5 uL of Mojosort Human  
457 Dead Cell Removal Beads (BioLegend) for one round bead depletion, or 5 uL of Mojosort  
458 Human Dead Cell Removal Beads and 5 uL of Mojosort Human anti-PE Nanobeads  
459 (BioLegend) for two round bead depletion. Samples were incubated with magnetic beads for 15  
460 minutes (4°C). Samples stained in tubes were washed with 3 mL of Mojosort Isolation Buffer,  
461 moved to a 5 mL tube magnet (Biolegend), and incubated for 3 minutes. Samples stained in  
462 plate format were washed with 150 uL of Mojosort Isolation Buffer, moved to a plate magnet  
463 adapter (Alpaqua), and incubated for 3 minutes. After transferring the supernatant to a new tube,  
464 the remaining beads were washed and magnetically depleted a second time. For samples  
465 undergoing two round depletion, the enriched cells were centrifuged at 400g for 5 min (4°C),  
466 stained a second time with 5 uL of Mojosort Human Dead Cell Removal Beads and 5 uL of  
467 Mojosort Human anti-PE Nanobeads, and magnetically enriched on the plate magnet two  
468 additional times. Enriched cells were centrifuged at 400g for 5 min (4°C) and resuspended in  
469 280 uL of Dulbecco's phosphate-buffered saline (DPBS). 30 uL of each sample was stained 1:1  
470 with 30 uL of AO/PI solution and counted on a Nexcelom Cellaca MX cell counter (Supplement  
471 Note). Plate format bead isolation and cell counting pipetting steps completed using a Tecan  
472 Fluent 1080 liquid handling automation system (Supplement Note).

473 10x Chromium Flex scRNA-seq and scCITE-seq

474 PBMC enriched samples were processed according to the 10x Genomics protocol for Fixation  
475 of Cells and Nuclei (CG000478, Rev C). Volumes were scaled from 1 mL to 250  $\mu$ L for plate-  
476 based sample preparation and handling. Prior to fixation, samples were stained using  
477 BioLegend's TotalSeq™-C Human Universal Cocktail(Cat. No 399905) according to the  
478 TotalSeq™-B or -C with 10x Feature Barcoding Technology protocol. Following extracellular  
479 protein staining, samples were fixed in a final concentration of 4% Paraformaldehyde for 1 hour  
480 (25°C). Fixed samples were quenched and subsequently washed with an additional 200  $\mu$ L of  
481 PBS + 0.02% BSA (Costar). Samples were barcoded for multiplexing using 10X Genomics  
482 Fixed RNA Feature Barcode Multiplexing Kit (PN-1000628). Probe hybridization was completed  
483 according to the 10x Genomics protocol for Multiplexed samples with Feature Barcode  
484 technology for Protein using Barcode Oligo Capture (CG000673, Rev A). Up to 2 million fixed  
485 cells were hybridized per sample. After 16-24 hours of probe hybridization incubation (42°C),  
486 samples were diluted in Post-Hyb Wash buffer and 11  $\mu$ L was removed for counting. The  
487 counting fraction was stained 1:5 with 44  $\mu$ L of PI solution and counted on a Nexcelom Cellaca  
488 MX cell counter (Supplement Note). Samples were then pooled at equivalent cell  
489 concentrations, incubated for 3 rounds of 10 minutes at 42°C, washed in Post-Hyb wash buffer,  
490 and strained using 30  $\mu$ M strainers (Miltenyi). The single cell suspension pool was loaded onto  
491 Chip Q for GEM generation at an overloaded concentration of 400,000 cells. Final scRNAseq  
492 libraries were sequenced using a NovaSeq X 25B PE300 or NovaSeq S4 PE100 flow cell,  
493 targeting a read depth of 10,000 reads per cell.

494 10x Chromium 3' v3.1 scRNA-seq

495 PBMC enriched samples were processed with the 10X Genomics Chromium Next Gem Single  
496 Cell 3' kit (v3.1) using a previously published protocol<sup>25</sup> ([Genge et al. 2021](#)). Samples were

497 stained with cell hashing antibodies and combined into pools of 12 samples. Pooled samples  
498 were then added to 10x Chromium Controller Chip G in replicate at a concentration of ~64,000  
499 cells per well across 12 wells. Generated libraries were sequenced on Illumina Novaseq using  
500 an S4 flowcell with 45k reads per cell for RNA libraries and 3k reads per cell for HTO libraries.

501 **Bulk ATAC-seq**

502 PBMC enriched samples were first permeabilized using 0.1% digitonin. Tagmentation reactions  
503 using Tagment DNA TDE1 Enzyme and Buffer Kit (Illumina, PN 20034198) were carried out on  
504 50,000 cells incubated for one hour at 37°C. DNA products were purified using a DNA Clean-Up  
505 buffer containing 0.1% SDS, 16 mM EDTA, 160 ug Proteinase K (ThermoFisher, PN EO0491),  
506 23 ug RNase A (ThermoFisher, PN EN0531) and incubated at 37°C overnight, followed by a  
507 1.8X AMPure XP bead selection (Beckman Coulter). DNA products were barcoded with a  
508 unique i7 primer and an universal i5 primer<sup>26,27</sup> and purified using a 0.4X right-sided and 1.2X  
509 left-sided AMPure XP bead clean up. Libraries were sequenced using a NextSeq2000 P2 PE50  
510 flow cell, with a sequencing depth of 10,000,000 reads per library.

511 **PBMC Stimulation**

512 PBMC enriched samples were resuspended in complete RPMI (Roswell Park Memorial Institute  
513 1640 media + 10% Fetal Bovine Serum + 1% Penicillin Streptomycin, Gibco) and plated in a 96  
514 well U bottom plate at a concentration of 500,000 cells per well. Cells were rested for 1 hour at  
515 37°C, and then exposed to one of four stimulation conditions: no stimulation, phorbol 12-  
516 myristate 13-acetate (PMA) (125 ng/mL, Fisher Scientific) with ionomycin (2.5 µg/mL, Fisher  
517 Scientific), resiquimod (R848) (500 ng/mL, Invivogen), or CD3/CD28 T cell activation beads (0.5  
518 beads/cell, Gibco). Cells were incubated for 4 hours at 37°C, then resuspended in 4% PFA for  
519 fixation and subsequent 10x Flex scRNA-seq analysis.

520 scRNA-seq and scCITE-seq Analysis

521 FASTQ files were used in the Cell Ranger (10x Genomics, v7.1.0) alignment function against  
522 the human reference annotation (Ensembl GRCh38). 10x Flex scRNA-seq and scCITE-seq  
523 matrices were generated using Cell Ranger Multi (10x Genomics, v7.1.0). 10x 3' v3.1 scRNA-  
524 seq matrices were processed using Cell Ranger, as described in [Savage et al. 2021](#)<sup>8</sup> and  
525 [Swanson et al. 2021](#)<sup>28</sup>. Cell doublets were identified in the data using Scrublet (v0.2.3)<sup>33</sup>  
526 Filtered cell by gene matrices were processed using Scrublet and saved to a comma separated  
527 value (csv) file with cell barcode, doublet score and doublet classification. Filtered cell by gene  
528 matrices were read into Seurat (Satija Lab, v5.1.0) with the Scrublet results to remove doublets  
529 from the analysis. Datasets were further filtered to remove cells with greater than 5% of  
530 mitochondrial gene expression.

531

532 To analyze scRNA-seq data, the filtered matrices were normalized (NormalizeData function,  
533 default settings), scaled (ScaleData function, defaults), and analyzed with principal component  
534 analysis (PCA) (RunPCA function, defaults). UMAPs (RunUMAP, dims = 1:20) and clustering  
535 analysis (FindClusters, resolution = 0.5, FindNeighbors, dims = 1:20) were also completed using  
536 the Seurat package. For label transfer, SCTransform was used to normalize the data in order to  
537 match the Seurat Multimodal Reference Dataset for PBMCs (available from the Satija lab at  
538 [https://atlas.fredhutch.org/data/nygc/multimodal/pbmc\\_multimodal.h5seurat](https://atlas.fredhutch.org/data/nygc/multimodal/pbmc_multimodal.h5seurat), Hao et al., 2020).  
539 Label transfer was then performed using the Seurat functions FindTransferAnchors and  
540 TransferData as described in the Seurat v4 Vignettes. Reference labels were mapped in the  
541 'celltype.l1' categories onto the filtered datasets. Cells labeled as celltype "other" was dropped  
542 from further analysis. For ADT counts, the filtered matrices were normalized (NormalizeData  
543 function, normalization.method='CLR', margin = 2), scaled (ScaleData function, defaults), and  
544 analyzed with principal component analysis (PCA) (RunPCA function, defaults). UMAPs

545 (RunUMAP, dims = 1:20) and clustering analysis (FindClusters, resolution = 0.5, FindNeighbors,  
546 dims = 1:20) were also completed using the Seurat package. Variance decomposition was  
547 performed using the PALMO package as described in Vasaiker et al. 2023 [21]. Processed  
548 Seurat objects for all data types were saved as .rds files for plotting.

## 549 Bulk ATAC-seq Analysis

550 Bulk ATAC-Seq samples were run through an internal bulk ATAC-Seq analysis pipeline in which  
551 each read pair is aligned to hg38 using bowtie2 (v2.4.5, available at  
552 <https://github.com/BenLangmead/bowtie2>). Results are written out to a SAM file and used to  
553 create a corresponding BAM file using samtools and a sorted BED file using bedtools for  
554 downstream analysis. To compare fragment length distributions between donors and sample  
555 conditions, the BED files are used to calculate fragment widths and fraction of total reads.  
556 Sorted BED files are randomly downsampled to 14 million reads and converted to BedGraph  
557 files as an intermediate to convert to BigWig files to complete genome track comparisons. The  
558 downsampled BED files are also used to examine transcription start site footprint position and  
559 coverage overlap using GRanges and IRanges relative to 2kb upstream and downstream of the  
560 TSS. Genome track plots were generated using Integrative Genomics Viewer<sup>34</sup>.

## 561 Statistical Analysis

562 Pearson correlation coefficients and p-values for cell frequency, gene expression, and protein  
563 expression comparisons across all figures were calculated using the *cor* and *cor.test* functions  
564 in the *stats* base package (v3.6.2) in the R statistical programming language (v4.3.3).

## 565 Abbreviations

566 ADT: Antibody derived tag

567 CryoSCAPE: Cryopreservation for Scalable Cellular And Protein Exploration  
568 CWB: Cryopreserved whole blood  
569 DC: Dendritic Cells  
570 DEG: Differentially expressed gene  
571 DMSO: Dimethyl sulfoxide  
572 DPBS: Dulbecco's phosphate-buffered saline  
573 EDTA: Ethylenediaminetetraacetic acid  
574 FACS: Fluorescence activated cell sorting  
575 IRB: Institutional review board  
576 NK: Natural killer  
577 PBMC: Peripheral blood mononuclear cell  
578 RBC: Red blood cell  
579 TSS: Transcriptional start site  
580 UMAP: Uniform manifold approximation and projection  
581 UMI: Unique molecular identifier

## 582 References

583 1. Derbois, Céline, Marie-Ange Palomares, Jean-François Deleuze, Eric Cabannes, and  
584 Eric Bonnet. 2023. "Single Cell Transcriptome Sequencing of Stimulated and Frozen  
585 Human Peripheral Blood Mononuclear Cells." *Scientific Data* 10 (1): 433.

586 2. Perkel, Jeffrey M. 2021. "Single-Cell Analysis Enters the Multiomics Age." *Nature* 595  
587 (7868): 614–16.

588 3. Sen, Partho, Esko Kemppainen, and Matej Orešič. 2017. "Perspectives on Systems  
589 Modeling of Human Peripheral Blood Mononuclear Cells." *Frontiers in Molecular  
590 Biosciences* 4: 96.

591 4. Guillaumet-Adkins, A., Rodríguez-Esteban, G., Mereu, E., Mendez-Lago, M., Jaitin, D.  
592 A., Villanueva, A., Vidal, A., Martinez-Marti, A., Felip, E., Vivancos, A., Keren-Shaul, H.,  
593 Heath, S., Gut, M., Amit, I., Gut, I., & Heyn, H. (2017). Single-cell transcriptome  
594 conservation in cryopreserved cells and tissues. *Genome Biology*, 18(1), 45.

595 5. Verschoor, Chris P., Vikas Kohli, and Cynthia Balion. 2018. "A Comprehensive  
596 Assessment of Immunophenotyping Performed in Cryopreserved Peripheral Whole  
597 Blood." *Cytometry. Part B, Clinical Cytometry* 94 (5): 662–70.

598 6. Braudeau, Cecile, Nina Salabert-Le Guen, Justine Chevreuil, Marie Rimbert, Jerome C.  
599 Martin, and Regis Josien. 2021. "An Easy and Reliable Whole Blood Freezing Method  
600 for Flow Cytometry Immuno-Phenotyping and Functional Analyses." *Cytometry. Part B,*  
601 *Clinical Cytometry* 100 (6): 652–65.

602 7. Olson, Walter C., Mark E. Smolkin, Erin M. Farris, Robyn J. Fink, Andrea R. Czarkowski,  
603 Jonathan H. Fink, Kimberly A. Chianese-Bullock, and Craig L. Slingluff Jr. 2011.  
604 "Shipping Blood to a Central Laboratory in Multicenter Clinical Trials: Effect of Ambient  
605 Temperature on Specimen Temperature, and Effects of Temperature on Mononuclear  
606 Cell Yield, Viability and Immunologic Function." *Journal of Translational Medicine* 9  
607 (March): 26.

608 8. Savage, Adam K., Miriam V. Gutschow, Tony Chiang, Kathy Henderson, Richard Green,  
609 Monica Chaudhari, Elliott Swanson, et al. 2021. "Multimodal Analysis for Human Ex Vivo  
610 Studies Shows Extensive Molecular Changes from Delays in Blood Processing."  
611 *iScience* 24 (5): 102404.

612 9. Yi, Ping-Cheng, Luting Zhuo, Julie Lin, Calvin Chang, Audrey Goddard, and Oh Kyu  
613 Yoon. 2023. "Impact of Delayed PBMC Processing on Functional and Genomic Assays."  
614 *Journal of Immunological Methods* 519 (August): 113514.

615 10. Davis, Terry C., Connie L. Arnold, Glenn Mills, and Lucio Miele. 2019. "A Qualitative  
616 Study Exploring Barriers and Facilitators of Enrolling Underrepresented Populations in  
617 Clinical Trials and Biobanking." *Frontiers in Cell and Developmental Biology* 7 (April): 74.

618 11. Feyman, Yevgeniy, Frank Provenzano, and Frank S. David. 2020. "Disparities in Clinical  
619 Trial Access Across US Urban Areas." *JAMA Network Open* 3 (2): e200172.

620 12. Wohnhaas, Christian T., Germán G. Leparc, Francesc Fernandez-Albert, David Kind,  
621 Florian Gantner, Coralie Viollet, Tobias Hildebrandt, and Patrick Baum. 2019. "DMSO  
622 Cryopreservation Is the Method of Choice to Preserve Cells for Droplet-Based Single-  
623 Cell RNA Sequencing." *Scientific Reports* 9 (1): 10699.

624 13. Serra, Valentina, Valeria Orrù, Sandra Lai, Monia Lobina, Maristella Steri, Francesco  
625 Cucca, and Edoardo Fiorillo. 2022. "Comparison of Whole Blood Cryopreservation  
626 Methods for Extensive Flow Cytometry Immunophenotyping." *Cells* 11 (9).  
627 <https://doi.org/10.3390/cells11091527>.

628 14. Satpathy, Sarthak, Beena E. Thomas, William J. Pilcher, Mojtaba Bakhtiari, Lori A.  
629 Ponder, Rafal Pacholczyk, Sampath Prahalad, Swati S. Bhasin, David H. Munn, and  
630 Manoj K. Bhasin. 2023. "The Simple prEservatioN of Single cElls Method for  
631 Cryopreservation Enables the Generation of Single-Cell Immune Profiles from Whole  
632 Blood." *Frontiers in Immunology* 14 (November): 1271800.

633 15. Huang, Dezhi, Naya Ma, Xinlei Li, Yang Gou, Yishuo Duan, Bangdong Liu, Jing Xia, et  
634 al. 2023. "Advances in Single-Cell RNA Sequencing and Its Applications in Cancer  
635 Research." *Journal of Hematology & Oncology* 16 (1): 98.

636 16. Haque, Ashraful, Jessica Engel, Sarah A. Teichmann, and Tatio Lönnberg. 2017. "A  
637 Practical Guide to Single-Cell RNA-Sequencing for Biomedical Research and Clinical  
638 Applications." *Genome Medicine* 9 (1): 75.

639 17. Alhamdan, Fahd, Kristina Laubhahn, Christine Happle, Anika Habener, Adan C. Jirmo,  
640 Clemens Thölken, Raffaele Conca, et al. 2022. "Timing of Blood Sample Processing  
641 Affects the Transcriptomic and Epigenomic Profiles in CD4+ T-Cells of Atopic Subjects."  
642 *Cells* 11 (19). <https://doi.org/10.3390/cells11192958>.

643 18. Qu, Hui-Qi, Charly Kao, James Garifallou, Fengxiang Wang, James Snyder, Diana J.  
644 Slater, Cuiping Hou, et al. 2023. "Single Cell Transcriptome Analysis of Peripheral Blood  
645 Mononuclear Cells in Freshly Isolated versus Stored Blood Samples." *Genes* 14 (1).  
646 <https://doi.org/10.3390/genes14010142>.

647 19. García-Piñeres, Alfonso J., Allan Hildesheim, Marcus Williams, Matthew Trivett, Susan  
648 Strobl, and Ligia A. Pinto. 2006. "DNase Treatment Following Thawing of Cryopreserved  
649 PBMC Is a Procedure Suitable for Lymphocyte Functional Studies." *Journal of  
650 Immunological Methods* 313 (1-2): 209–13.

651 20. Cheng, Junyun, Jie Liao, Xin Shao, Xiaoyan Lu, and Xiaohui Fan. 2021. "Multiplexing  
652 Methods for Simultaneous Large-Scale Transcriptomic Profiling of Samples at Single-  
653 Cell Resolution." *Advancement of Science* 8 (17): e2101229.

654 21. Vasaikar, Suhas V., Adam K. Savage, Qiuyu Gong, Elliott Swanson, Aarthi Talla, Cara  
655 Lord, Alexander T. Heubeck, et al. 2023. "A Comprehensive Platform for Analyzing  
656 Longitudinal Multi-Omics Data." *Nature Communications* 14 (1): 1684.

657 22. Lin, Yingxin, Shila Ghazanfar, Dario Strbenac, Andy Wang, Ellis Patrick, David M. Lin,  
658 Terence Speed, Jean Y. H. Yang, and Pengyi Yang. 2019. "Evaluating Stably Expressed  
659 Genes in Single Cells." *GigaScience* 8 (9). <https://doi.org/10.1093/gigascience/giz106>.

660 23. Lee, Jung Ho, Brian H. Lee, Soyoung Jeong, Christine Suh-Yun Joh, Hyo Jeong Nam,  
661 Hyun Seung Choi, Henry Sserwadda, et al. 2023. "Single-Cell RNA Sequencing  
662 Identifies Distinct Transcriptomic Signatures between PMA/ionomycin- and  
663 αCD3/αCD28-Activated Primary Human T Cells." *Genomics & Informatics* 21 (2): e18.

664 24. Hanten, John A., John P. Vasilakos, Christie L. Riter, Lori Neys, Kenneth E. Lipson,  
665 Sefik S. Alkan, and Woubalem Birmachu. 2008. "Comparison of Human B Cell Activation  
666 by TLR7 and TLR9 Agonists." *BMC Immunology* 9 (July): 39.

667 25. Genge, Palak C., Charles R. Roll, Alexander T. Heubeck, Elliott Swanson, Nina Kondza,  
668 Cara Lord, Morgan Weiss, et al. 2021. "Optimized Workflow for Human PBMC Multiomic  
669 Immunosurveillance Studies." *STAR Protocols* 2 (4): 100900.

670 26. Buenrostro, Jason D., Paul G. Giresi, Lisa C. Zaba, Howard Y. Chang, and William J.  
671 Greenleaf. 2013. "Transposition of Native Chromatin for Fast and Sensitive Epigenomic  
672 Profiling of Open Chromatin, DNA-Binding Proteins and Nucleosome Position." *Nature  
673 Methods* 10 (12): 1213–18.

674 27. Buenrostro, Jason D., Beijing Wu, Howard Y. Chang, and William J. Greenleaf. 2015.  
675 "ATAC-Seq: A Method for Assaying Chromatin Accessibility Genome-Wide." *Current*

676        *Protocols in Molecular Biology / Edited by Frederick M. Ausubel... [et Al.]* 109 (January):

677        21.29.1–21.29.9.

678        28. Swanson, Elliott, Cara Lord, Julian Reading, Alexander T. Heubeck, Palak C. Genge,  
679            Zachary Thomson, Morgan D. A. Weiss, et al. 2021. “Simultaneous Trimodal Single-Cell  
680            Measurement of Transcripts, Epitopes, and Chromatin Accessibility Using TEA-Seq.”  
681            *eLife* 10 (April). <https://doi.org/10.7554/eLife.63632>.

682        29. Butler, Andrew, Paul Hoffman, Peter Smibert, Efthymia Papalex, and Rahul Satija.  
683            2018. “Integrating Single-Cell Transcriptomic Data across Different Conditions,  
684            Technologies, and Species.” *Nature Biotechnology* 36 (5): 411–20.

685        30. Hao, Yuhang, Stephanie Hao, Erica Andersen-Nissen, William M. Mauck 3rd, Shiwei  
686            Zheng, Andrew Butler, Maddie J. Lee, et al. 2021. “Integrated Analysis of Multimodal  
687            Single-Cell Data.” *Cell* 184 (13): 3573–87.e29.

688        31. Hao, Yuhang, Tim Stuart, Madeline H. Kowalski, Saket Choudhary, Paul Hoffman, Austin  
689            Hartman, Avi Srivastava, et al. 2024. “Dictionary Learning for Integrative, Multimodal and  
690            Scalable Single-Cell Analysis.” *Nature Biotechnology* 42 (2): 293–304.

691        32. Stuart, Tim, Andrew Butler, Paul Hoffman, Christoph Hafemeister, Efthymia Papalex,  
692            William M. Mauck 3rd, Yuhang Hao, Marlon Stoeckius, Peter Smibert, and Rahul Satija.  
693            2019. “Comprehensive Integration of Single-Cell Data.” *Cell* 177 (7): 1888–1902.e21.

694        33. Wolock, Sam. n.d. *Scrublet: Detect Doublets in Single-Cell RNA-Seq Data*. Github.  
695            Accessed June 3, 2024. <https://github.com/swolock/scrublet>.

696        34. Helga Thorvaldsdóttir, James T. Robinson, Jill P. Mesirov. Integrative Genomics Viewer  
697            (IGV): high-performance genomics data visualization and exploration. *Briefings in  
698            Bioinformatics* 14, 178–192 (2013).

## 699 Declarations

### 700 Ethics approval and consent to participate

701 Specimens purchased from Bloodworks NW were collected under BloodWorks WIRB Protocol  
702 #20141589. Specimens provided by Benaroya Research Institute were collected under  
703 Benaroya Research Institute IRB #IRB19-045. All sample collections were conducted by  
704 Bloodworks NW and Benaroya Research Institute under these IRB protocols, and all donors  
705 signed informed consent forms.

### 706 Consent for publication

707 Not applicable.

### 708 Data Availability

709 Raw 10x Flex scRNA-seq data has been deposited in SRA (accession number #  
710 SUB14488403). Raw 10x 3' v3.1 scRNAseq data are deposited dbGaP for controlled access  
711 (dbGaP study accession #). Processed scRNA-seq (10x Flex and 10x 3' v3.1), scCITE-seq, and  
712 bulk ATAC data has been deposited in GEO (accession number #). All graphical figures created  
713 using Biorender.com. Data processing notebooks are available via Zenodo  
714 (10.5281/zenodo.11479595). Analysis code is available on Github  
715 ([https://github.com/aifimmunology/CWB\\_Paper](https://github.com/aifimmunology/CWB_Paper)).

### 716 Competing Interests

717 The authors have no competing interests to disclose.

### 718 Funding

719 No external funding was received for this research.

720 **Authors' contributions**

721 A.H., C.P., N.K., P.W., J.G., M.W., and P.S. designed the experiments, analyzed the data and  
722 prepared the manuscript. P.G. processed ATAC-seq data and provided bioinformatics support.  
723 Z.T., C.G., and J.R., provided experimental, analysis, and editing support.

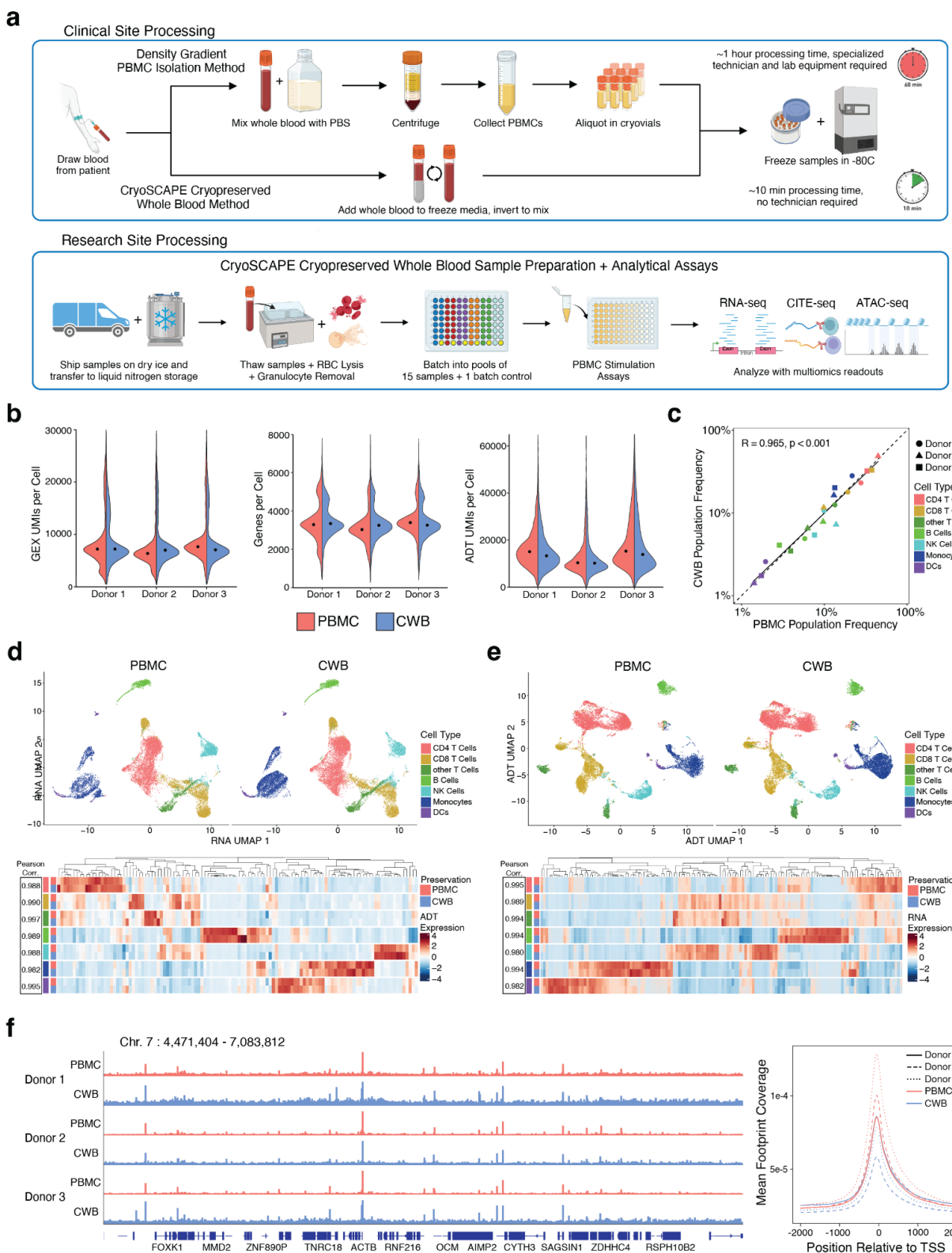
724 **Acknowledgments**

725 The authors are grateful to the donors that provided biological material for this study. The  
726 authors would like to thank the members of the Allen Institute for Immunology, especially the  
727 Lab Operations team who helped facilitate this research, as well as the Human Immune System  
728 Explorer (HISE) software development team for their support. The authors also thank the Allen  
729 Institute founder, Paul G. Allen, for his vision, encouragement, and support.

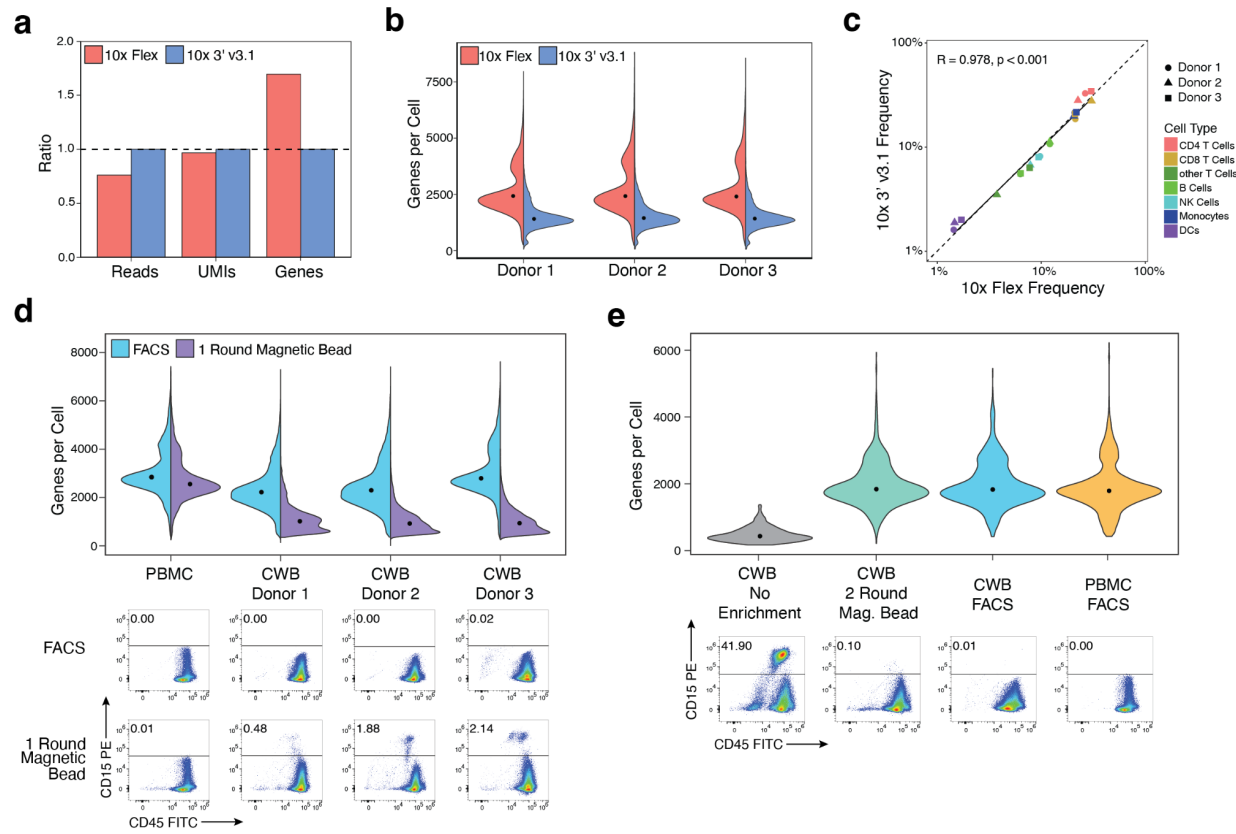
730 **Corresponding authors**

731 Correspondence to Alexander Heubeck ([alex.heubeck@alleninstitute.org](mailto:alex.heubeck@alleninstitute.org)) and Peter Skene  
732 ([peter.skene@alleninstitute.org](mailto:peter.skene@alleninstitute.org)).

733 **Figures**



735 **Figure 1: Whole blood cryopreservation in comparison to density gradient isolated PBMC**  
736 **cryopreservation for clinical site processing and multi-modal sequencing assays. a.**  
737 Schematic of clinical site processing for whole blood cryopreservation versus density gradient  
738 isolated PBMC cryopreservation demonstrating reduced processing time and workflow  
739 complexity. **b.** scRNAseq data quality metrics from individual donors with density gradient  
740 isolated PBMCs (red) and cryopreserved whole blood (blue) including gene expression (GEX)  
741 unique molecular identifiers (UMIs) per cell, genes per cell, and antibody derived tag (ADT)  
742 UMIs per cell. **c.** Correlation of cell type population frequencies between donor matched  
743 cryopreserved whole blood and density gradient isolated PBMC samples (Dashed line:  $R=1$ ,  
744 solid line: regression line,  $R=0.97$ ,  $p<0.001$ ). **d.** (Top) UMAP visualization of gene expression  
745 from cryopreserved whole blood and density gradient isolated PBMC samples overlaid with cell  
746 type labels. (Bottom) Relative gene expression levels for the highest expressing genes per cell  
747 type each cryopreservation method. High correlation is measured for each cell type indicating  
748 consistent gene detection between methods ( $R>0.979$ ,  $p<0.001$ ). **e.** (Top) UMAP visualization of  
749 ADT protein expression from cryopreserved whole blood and density gradient isolated PBMC  
750 samples overlaid with cell type labels. (Bottom) ADT expression levels for each  
751 cryopreservation method. High correlation is measured for each cell type indicating consistent  
752 protein detection between methods ( $R>0.981$ ,  $p<0.001$ ). **f.** (Left) Bulk ATAC-seq results  
753 showing a representative genome track (Chr. 7 : 4,471,404 - 7,083,812) with equivalent  
754 chromatin accessibility for cryopreserved whole blood and density gradient isolated PBMC  
755 samples across 3 donors. (Right) Distribution of footprints and position relative to TSS: total  
756 coverage of Tn5 footprints summed across all transcription start sites (TSS). Tn5 footprints are  
757 29 bp regions comprising the 9 bp target-site duplication (TSD) and 10 bp on either side, which  
758 represent accessible chromatin for each transposition event.

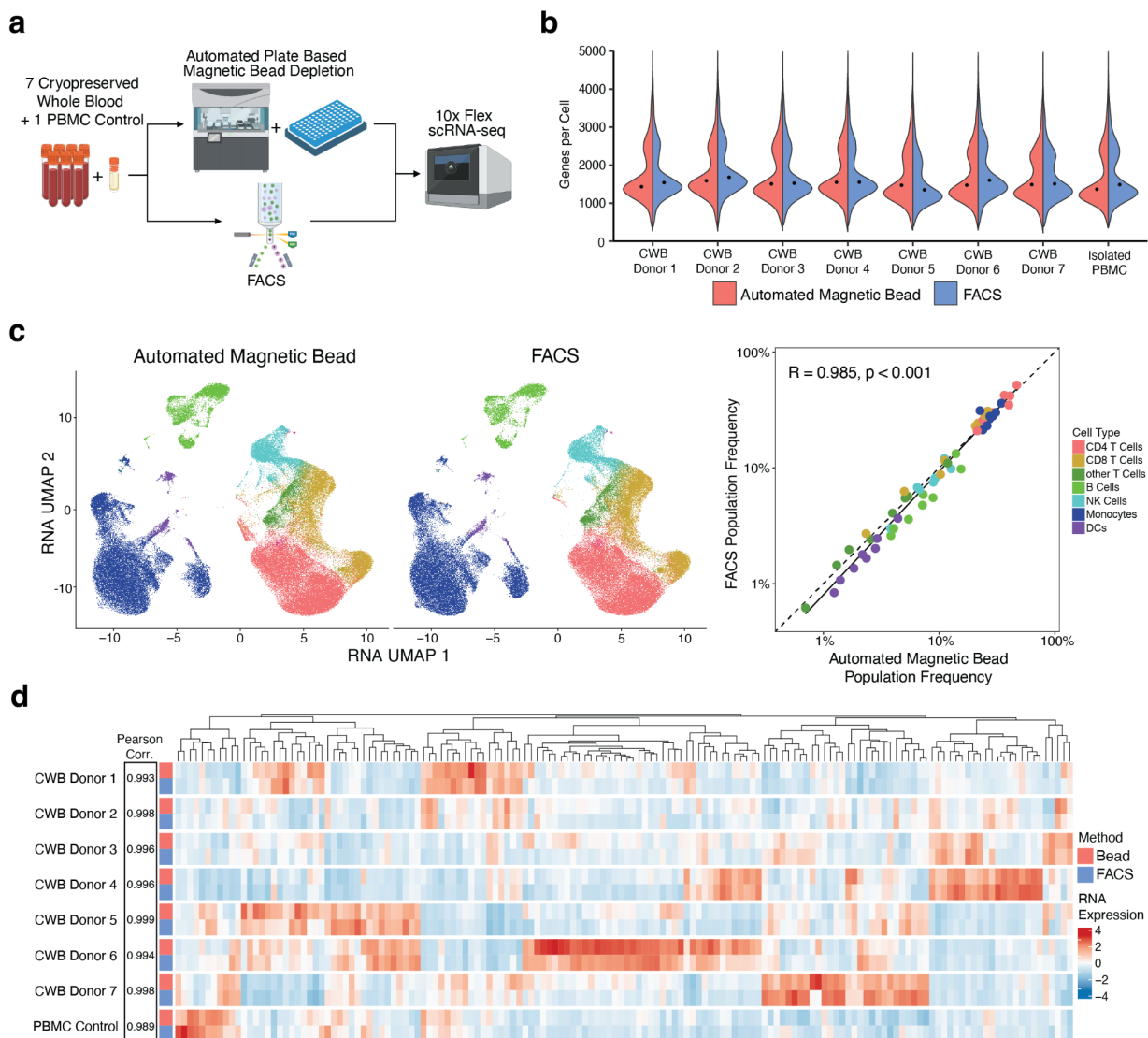


759

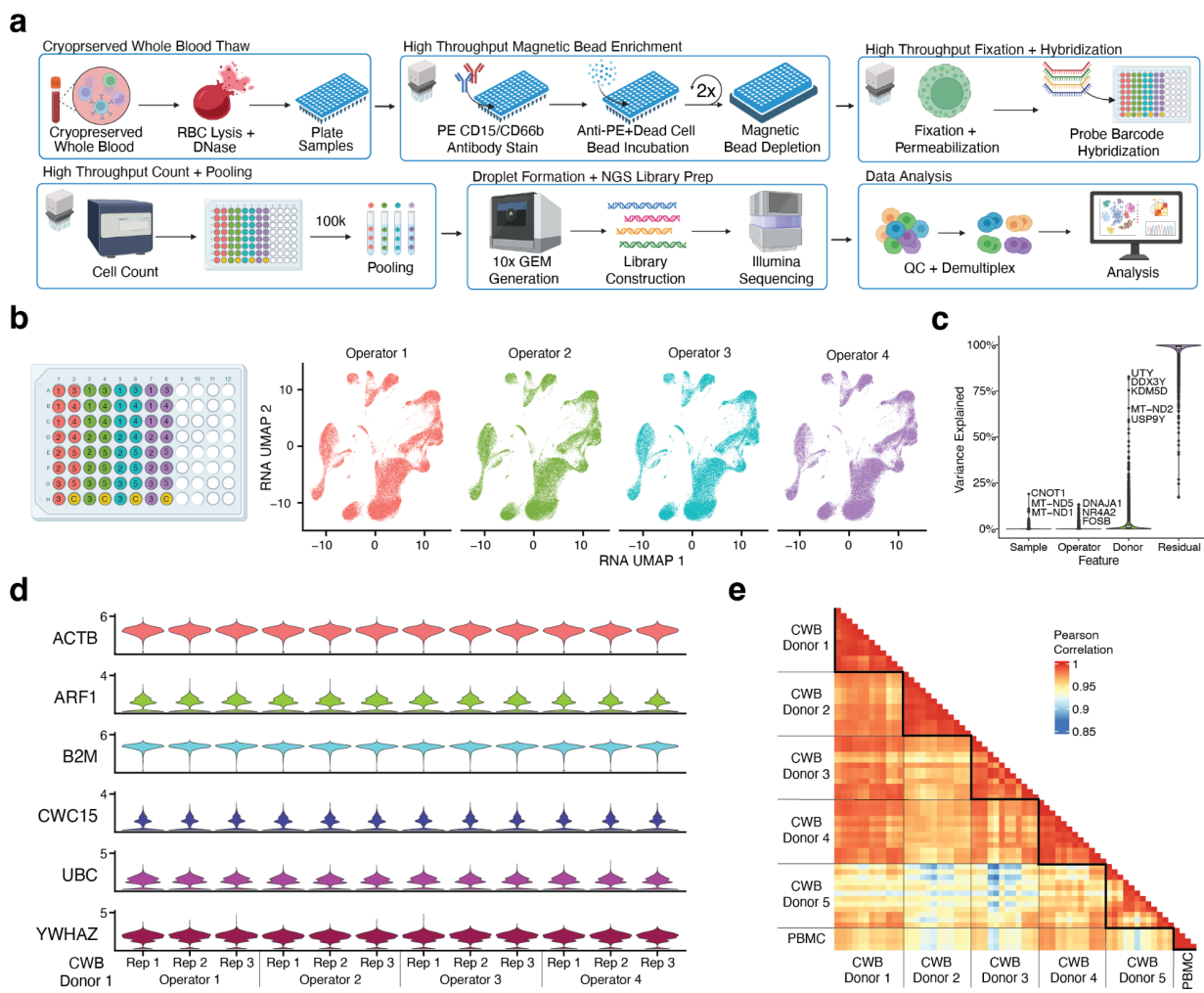
760 **Figure 2: Development of 10x Flex multiplexed scRNA-seq methodology as a high**  
761 **throughput method for single cell transcriptome analysis of cryopreserved whole blood.**

762 **a.** Ratio of 10x Flex (red) to 10x 3' v3.1 (blue) quality metrics comparing number of reads, UMs,  
763 and genes detected in scRNAseq libraries prepared from PBMC donors (n=3). **b.** Genes per cell  
764 recovered from individual donors (n=3) using 10x Flex and 10x 3' v3.1 methods. **c.** Correlation  
765 of cell type population frequencies between donor matched samples analyzed using 10x Flex  
766 and 10 3' v3.1 methods (Dashed line equivalent to  $R=1$ , solid line equivalent to regression line,  
767  $R=0.995, p < 0.001$ ). **d.** (Top) Genes per cell recovered using the 10x Flex kit with cryopreserved  
768 whole blood and density gradient isolated PBMC samples enriched using a single round of  
769 magnetic bead based enrichment (purple) versus FACS (blue). (Bottom) Remaining granulocyte  
770 contamination after enrichment by flow cytometry analysis. Relatively low numbers of  
771 granulocytes impact recovered genes per cell. **e.** (Top) Genes per cell recovered using the 10x

772 Flex kit with cryopreserved whole blood samples with no enrichment (gray), improved 2 round  
773 magnetic bead enrichment (green), and FACS (blue). Improved magnetic bead enrichment  
774 recover similar genes per cell compared to density gradient isolated PBMCs analyzed using the  
775 same kit (yellow). (Bottom) Remaining granulocyte contamination after enrichment by flow  
776 cytometry analysis. Improved magnetic bead enrichment removes granulocytes to a sufficient  
777 level.



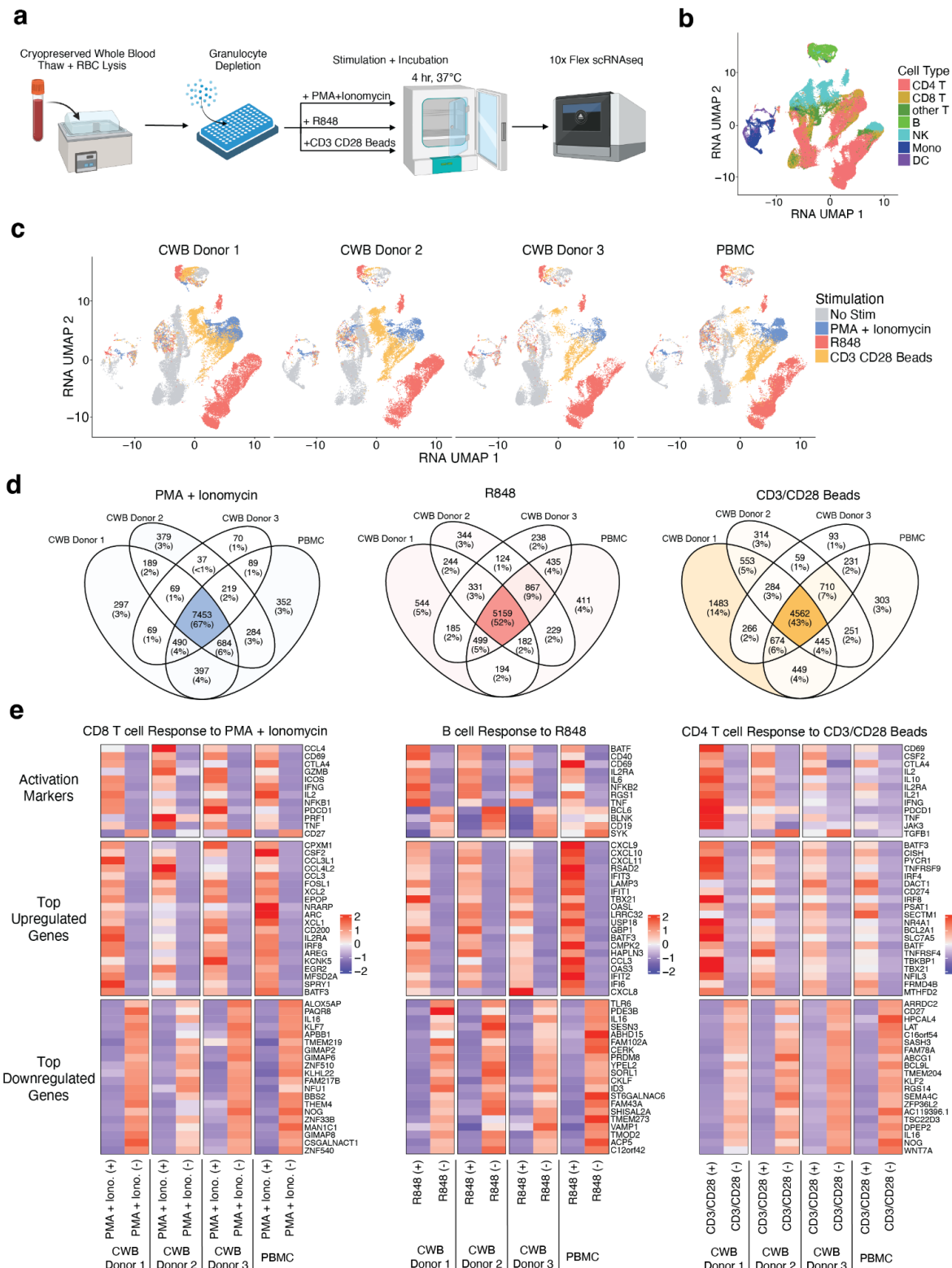
787 equivalent to R=1, solid line equivalent to regression line, R=0.988, p<0.001). **d.** Relative gene  
788 expression levels for the highest expressing genes per cell type for each enrichment method.  
789 High correlation was observed between donor replicates indicating consistent gene detection  
790 between methods (R>0.993).



791

792 **Figure 4: Verification of high throughput workflow with 60 cryopreserved whole blood**  
 793 **samples through automated magnetic bead enrichment and scRNA-seq preparation. a.**  
 794 Overview of complete cryopreserved whole blood processing workflow. **b.** (Left) Layout of batch  
 795 structure including 3 technical replicates of 5 donors across 4 thaw operators, and 1 PBMC  
 796 batch control across all 4 pools. (Right) UMAP visualizations of single cell gene expression  
 797 across each pool. **d.** Variance decomposition analysis evaluating contributions of sample  
 798 technical replicates, operator, and donor to total variance of individual genes. The vast majority  
 799 of variance in gene expression is not attributed to experimental variables **d.** Gene expression of  
 800 6 housekeeping genes across technical replicates from 1 donor, demonstrating high

801 consistency between thaw operators and sample tubes (CVs for all genes <5%). **e.** Average  
802 gene expression correlation between each sample, showing high consistency between technical  
803 replicates ( $R>0.96$ ).



805 **Figure 5: Functional assays using cryopreserved whole blood and multiplexed scRNA-**  
806 **seq. a.** Overview of experimental method for stimulation of cryopreserved whole blood samples  
807 with PMA + ionomycin, R848, and CD3/CD28 T cell activation beads. **b.** UMAP visualization of  
808 gene expression from stimulated cryopreserved whole blood samples overlaid with major cells  
809 types. Separate islands of the same cell type indicate divergent gene expression from different  
810 stimulation conditions. **c.** UMAP visualization of gene expression from stimulated cryopreserved  
811 whole blood samples overlaid with specific stimulation conditions. Cells from each donor cluster  
812 together in response to stimulation, demonstrating preservation of cellular response in  
813 cryopreserved whole blood. **c.** Venn diagrams showing overlapping differentially expressed  
814 genes (DEGs) from individual donors in response to each stimulation condition. The majority of  
815 DEGS are common in all donors. **e.** Relative gene expression of known activation markers and  
816 unsupervised DEGs from all donors in response to each stimulation condition. Similar activation  
817 patterns are seen in all donors.